Wavelet Analysis of Time Series for the Duffing Oscillator: The Detection of Order within Chaos

Delmar Permann and Ian Hamilton[a]

Department of Chemistry, The University of Ottawa, Ottawa, Canada K1N 9B4
(Received 26 December 1991)

We consider a wavelet analysis of various time series for the Duffing oscillator, for which there is a potential maximum and a harmonic forcing term, and we focus on time series that return to the region of the potential maximum. When the dynamics is chaotic and the time series is highly nonstationary, there are many significant higher harmonics in a Fourier expansion and the usual Fourier analysis is problematic, especially for short total times. We show that the wavelet analysis is a robust tool that may be used to obtain qualitative information for highly nonstationary time series—specifically, that it may be used to detect a small-amplitude harmonic forcing term even when the dynamics is chaotic and even for short total times.

The Fourier transform decomposes the time series of a variable using harmonic basis functions that are completely localized in frequency but completely delocalized in time. It is assumed [1] that the time series is stationary but this assumption is often invalid for actual signals. Recently, there have been extensive efforts, discussed by Priestly [2], to extend the Fourier transform to analyze nonstationary time series but, in general, these extensions also use harmonic basis functions (and examine power-series expansions in which correlations are introduced). The wavelet transform decomposes the time series of a variable using wavelet basis functions [3–10] that are localized in both frequency and time for a wide range of frequency and time scales. Wavelet basis functions were developed for the analysis of seismic signals [11] but have recently been used to analyze other signals (such as those connected with speech and vision) for which there are large variations in the frequency or time scales [12,13]. The wavelet basis functions used here are two-parameter functions that are an orthogonal basis for $L^2(R)$, and which are obtained from a single function by (one time unit) shifts that act on the time variable and (factor of 2) dilations that act on both the time and frequency variables. As discussed by Chiu [5] and Strang [10], the basic set of orthogonal wavelet basis functions was devised by Daubchies [6] and, from this set, we choose the relatively smooth eight-coefficient functions. The six- and ten-coefficient functions give very similar results but there is some sensitivity to function shape. The wavelet transform is termed a multiresolution decomposition because each stage of the decomposition uses a different resolution, and the difference between the approximations to the function at stages j and $j-1$ is termed the detail of the function at stage j. Our aim is to show that the wavelet transform is a robust tool that may be used to obtain qualitative information for highly nonstationary time series. Specifically, we consider time series for the Duffing Wscillator and we examine details of these time series at several stages. We show that the wavelet transform may be used to detect a small-amplitude harmonic forcing term in the sense that the periodicity is evident

for certain details.

A wavelet transform and a windowed (or short-time) Fourier transform [1,4,5] are similar in that both perform a frequency analysis of the time series locally. However, for a windowed Fourier transform, the time resolution is the same for all frequencies whereas for a wavelet transform, the time resolution is sharper for higher frequencies. Consequently, a wavelet analysis can more easily detect a high-frequency component of the time series. Therefore, a wavelet analysis may be a valuable (if not indispensable) complement to a windowed Fourier analysis, especially for short total times. This is significant since the signal to be analyzed may only be available for short total times. A wavelet transform and a filtered Fourier transform [1,7,8] are similar in that both can be used to isolate frequency bands from the time series— in the extreme case, a comb filter can be used to isolate a single frequency. However, for the wavelet transform, the procedure is systematic and no information is lost —the time series can be both decomposed and reconstructed. The wavelet transform used here is discrete and is analogous to, and at least as efficient as, the last Fourier transform. It employs a pyramidal algorithm, developed by Mallat [9], that is briefly discussed later.

For the Duffing oscillator considered here the potential energy is [14]

$$V = x^4/4 - x^2/2. \tag{1}$$

Thus there are two identical wells separated by a potential maximum at $x=0$. The equation of motion for the Duffing oscillator considered here is [14]

$$\ddot{x} = x - x^3 - \delta\dot{x} + \gamma\cos(\omega t). \tag{2}$$

The Duffing oscillator was developed as a simple model for the hardening spring effect in many mechanical systems but has become one of the most common examples of a nonlinear oscillator [15] and is briefly considered by Priestly [1].

When a system is in the linear regime a Fourier analysis of the time series is efficient. However, when a system is in the nonlinear regime there are many

significant higher harmonics in a Fourier expansion, and the usual Fourier analysis is problematic in a practical sense. This is especially true for short total times as a Fourier analysis has difficulty distinguishing low-amplitude peaks from noise for the kinds of nonstationary signals under consideration. For simplicity we choose $x(0) = 0.0$ and, having specified the initial total energy $E(0)$, we solve for $\dot{x}(0) = -[2E(0)]^{1/2}$. Here we choose $E(0) = 10^{-5}$ so $x(0)$ is in the region of the potential maximum (at $x = 0$) and (for small γ) the time series returns to this region. Although γ is small, it may have a strong effect and the dynamics may be chaotic [16] for some parameter values. It is then necessary to use an accurate numerical integrator and here we use the well-tested predictor-corrector method of Gear [17]. Here it is assumed that $x(t)$ is known to five significant figures (issues related to finite precision and interactive noise will be considered in a future publication).

We first briefly consider some mathematical properties [3–10] of the wavelet basis functions and the corresponding subspaces of $L^2(R)$. The V_m are subspaces of L^2 such that their union is L^2 but their intersection is not null. W_m is defined to be the orthogonal complement of V_m in V_{m-1} (and V_{m-1} is the direct sum of V_m and W_m). Thus each V_m is a subset of V_{m-1} and its principal property is that if $g(t)$ is an element of V_m then $g(2t)$ is an element of V_{m-1}. It is possible to define two-parameter functions $\phi_{mn}(t) = 2^{-m/2}\phi(2^{-m}t - n)$ that are basis functions for V_m and two-parameter functions $\psi_{mn}(t) = 2^{-m/2}\psi(2^{-m}t - n)$ that are basis functions for W_m. The W_m are subspaces of L^2 such that their union is L^2 and their intersection is null. Thus the $\psi_{mn}(t)$ are an orthogonal basis for L^2 and these are the wavelet basis functions used here.

We now briefly consider the algorithm, developed by Mallat [9], that is used for the decomposition of $f(t)$. Here the c_n^0 are the 2^N values of $f(t)$ that comprise the time series and there are N stages in the decomposition. The first stage is $f = A_1 f + D_1 f$ while the jth stage is

$$A_{j-1}f = A_j f + D_j f \tag{3}$$

with

$$A_j f = \sum_k c_k^j \phi_{jk} \tag{4}$$

and

$$D_j f = \sum_k d_k^j \psi_{jk}, \tag{5}$$

where the coefficients c_k^j and d_k^j are defined recursively. Here the d_k^j are the coefficients of the detail of f at stage j which are considered below. The above algorithm is pyramidal and requires a minimum number of operations since at each stage only half the values of $f(t)$ need be retained. For the reconstruction of $f(t)$ essentially the same formulas are used in reverse. Therefore, while the first stage in the decomposition is at the highest resolution, the first stage in the reconstruction is at the lowest resolution.

We examine details of $x(t)$ at several stages for a certain time interval. In this time interval $A_j x(t)$ is a fuzzy approximation of $x(t)$ at stage j. $A_{j-1}x(t)$ is a less fuzzy approximation of $x(t)$ at stage $j-1$ which can be reconstructed from $A_j x(t)$ and $D_j x(t)$. $D_j x(t)$, which is discrete, is termed the detail of $x(t)$ at stage j (or simply detail j) and is the difference between the approximations to $x(t)$ at stages j and $j-1$. Thus, in a given time interval, the amplitude of $D_j x(t)$ is proportional to the difference between $A_j x(t)$ and $A_{j-1}x(t)$ in this time interval. Here this amplitude is plotted and, to guide the eye, the points are joined by straight-line segments with no smoothing.

Unless otherwise stated, results are for total time 120. We consider $x(t)$ and details of $x(t)$ at several stages for $t = 26$ to 32 (our motivation for choosing this time interval is indicated below). We first consider results for $\gamma = 1.0 \times 10^{-3}$. Figures 1(a) and 1(b) show $x(t)$ from $t = 0$ to 120 for $\omega = 8.0$ and 4.0, respectively. It may be seen that the dynamics appears regular for $\omega = 8.0$ and chaotic for $\omega = 4.0$ and this is confirmed by calculations of the Lyapunov exponent [15] which (for base 10) is obtained from the average rate of increase of $\lambda(t)$ $= \log_{10} d(t)$. Figures 1(c) and 1(d) show $\lambda(t)$ with $d(0)$ $= 10^{-12}$ for $\omega = 8.0$ and 4.0, respectively. It may be seen that although $\lambda(t)$ is highly oscillatory in both cases, the average rate of increase is essentially zero for $\omega = 8.0$ and positive for $\omega = 4.0$. The total time 0 to 120 was divided into 8192 steps and the thirteen details of $x(t)$ were obtained for $t = 0$ to 120 (note that detail 1 has 4096 points and detail 13 has 1 point). Figure 2(a) shows $x(t)$ (with vertical scale expanded) for $\omega = 8.0$ while Figs. 2(b), 2(c), and 2(d) show details 2, 3, and 4, respectively (note that for successive details the vertical scale increases by
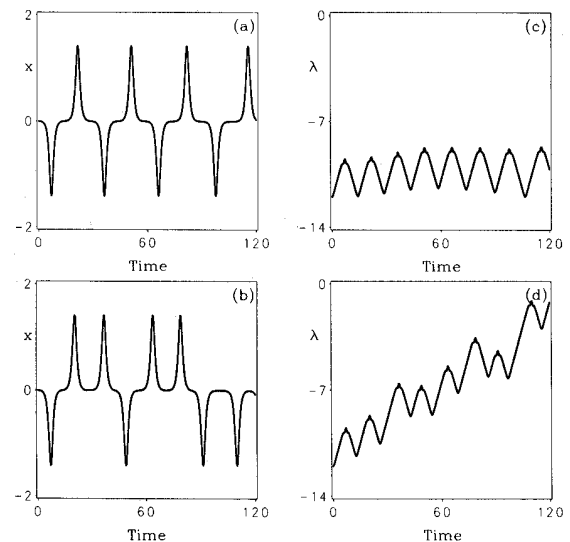
FIG. 1. For $t = 0$ to 120 and $\gamma = 1.0 \times 10^{-3}$: (a) $x(t)$ vs t for $\omega = 8.0$; (b) $x(t)$ vs t for $\omega = 4.0$; (c) $\lambda(t)$ vs t for $\omega = 8.0$; (d) $\lambda(t)$ vs t for $\omega = 4.0$.
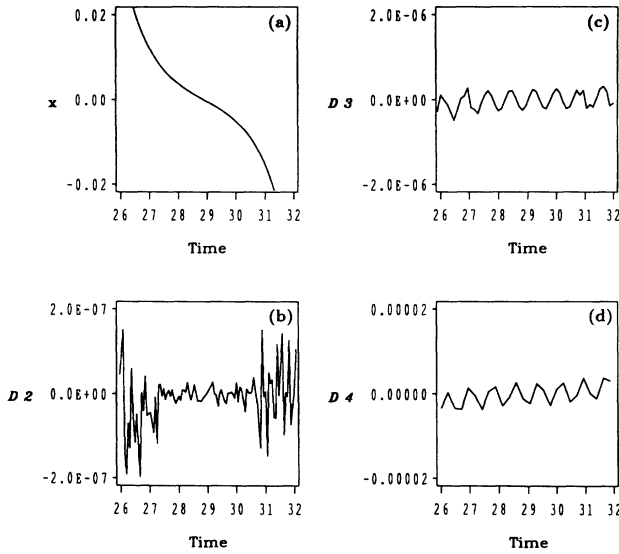
FIG. 2. For $\omega = 8.0$, $\gamma = 1.0 \times 10^{-3}$, and total time 120: (a) $x(t)$ vs t; (b) detail 2; (c) detail 3; (d) detail 4.
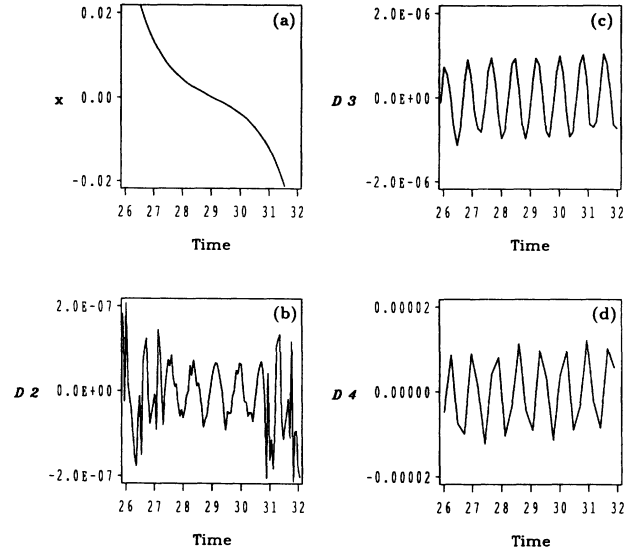
FIG. 4. Same as for Fig. 2 but for $\gamma = 4.0 \times 10^{-3}$.

an order of magnitude). It may be seen that detail 3 [Fig. 2(c)] is predominantly periodic with approximate period $\pi/4$, as anticipated for $\omega = 8.0$. Detail 2 [Fig. 2(b)] is completely "noisy" as is detail 1, which is not shown. This periodicity is somewhat evident in detail 4 [Fig. 2(d)] which is jagged as there are half as many points as in Fig. 2(c). Figure 3(a) shows $x(t)$ (with vertical scale expanded) for $\omega = 4.0$ while Figs. 3(b), 3(c), and 3(d) show details 2, 3, and 4, respectively (note that for each detail the vertical scale is a factor of 4 smaller than in Fig. 2). It may be seen that detail 3 [Fig. 3(c)] is predominantly periodic with approximate period $\pi/2$, as anticipated for $\omega = 4.0$. Detail 2 [Fig. 3(b)] is completely

"noisy" but this periodicity is evident in detail 4 [Fig. 3(d)] as there are as many points as in Fig. 2(d) but the approximate period is double. Thus, the wavelet transform may be used to detect a small-amplitude harmonic forcing term even when the dynamics is chaotic. Note that, especially when the dynamics is chaotic, it is not possible to do this by subtracting from $x(t)$ the periodic time series for $\delta = 0$ and $\gamma = 0$, and the harmonic forcing term is not evident in $x(t)$ for this time interval even with the vertical scale expanded [Fig. 3(a)].

We now consider results for $\gamma = 4.0 \times 10^{-3}$. Figure 4(a) shows $x(t)$ (with vertical scale expanded) for $\omega = 8.0$ while Figs. 4(b), 4(c), and 4(d) show details 2, 3, and 4, respectively (note that for each detail the vertical scale is the same as in Fig. 2). It may be seen that detail 3 [Fig. 4(c)] is predominantly periodic with period $\pi/4$, as in Fig. 2(c), but the amplitude is approximately 4 times that in Fig. 2(c). Detail 2 [Fig. 2(b)] is "noisy" but this periodicity is evident for part of the time interval. This periodicity is somewhat evident in detail 4 [Fig. 4(d)] which is jagged as there are half as many points as
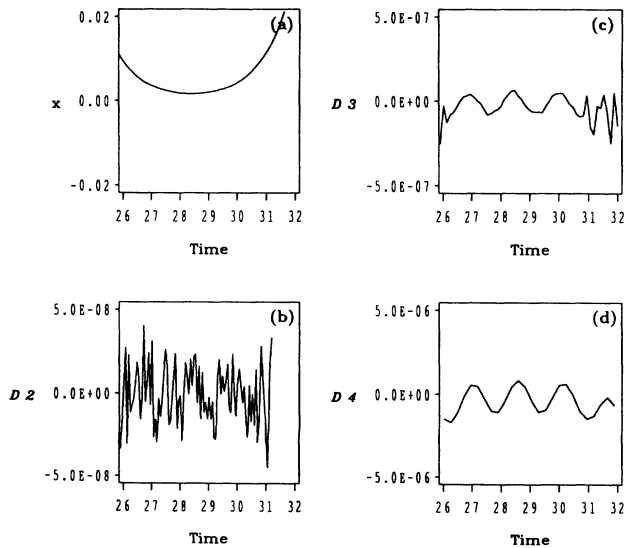
FIG. 3. Same as for Fig. 2 but for $\omega = 4.0$.
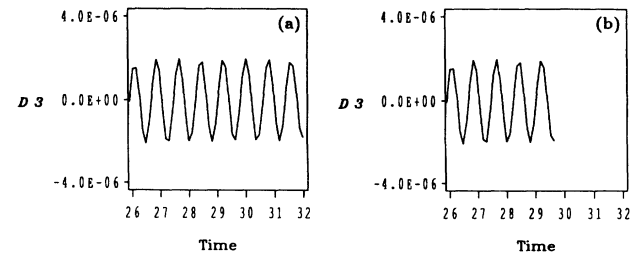
FIG. 5. Detail 3 for $\omega = 0$, $\gamma = 8.0 \times 10^{-3}$, and total time (a) 60, (b) 30.

2609

in Fig. 4(c).

Finally, we consider results for shorter total times for $\gamma = 8.0 \times 10^{-3}$ and $\omega = 8.0$. Figures 5(a) and 5(b) show detail 3 for total times 60 and 30 divided into 4096 and 2048 steps, respectively [note that the vertical scale is a factor of 2 larger than in Fig. 2(c)]. It may be seen that detail 3 is predominantly periodic with approximate period $\pi/4$, as in Fig. 2(c), but the amplitude is approximately 8 times that in Fig. 2(c). This is the case even for Fig. 5(b) where, for total time 30, detail 3 exists for only part of the time interval 26 to 32 (which is our motivation for choosing this time interval). For total times 60 and 30 divided into 8192 and 4096 steps, respectively, the details are essentially the same but at a stage one higher — the relevant quantity is the density of points for the time interval. The details are not exactly the same because there are edge effects but, because the wavelet basis functions are localized in time, these effects are minimal. The periodicity is evident for certain details when the corresponding wavelet basis functions have the appropriate localization in both frequency and time for the time interval. As shown here, this resolution requires a relatively slow rate of change of $x(t)$ for the time interval. Thus, for example, the wavelet analysis also works well for $t = 11$ to 17 or 40 to 46 but not for $t = 18$ to 24 or 33 to 39 [where, for most of the time interval, $x(t)$ is increasing or decreasing rapidly]. The point we wish to emphasize is that the wavelet analysis is a robust tool that is practical and efficient even when the dynamics is chaotic and even for short total times. This is significant since the signal to be analyzed may only be available for short total times.

---

[a]Present address: Department of Chemistry, Wilfrid Laurier University, Waterloo, Canada N2L 3C5.

[1] M. B. Priestly, Spectral Analysis and Time Series (Academic, London, 1981).

[2] M. B. Priestly, Non-linear and Non-stationary Time Series Analysis (Academic, London, 1988).

[3] Y. Meyer, Ondelettes (Hermann, Paris, 1990).

[4] I. Daubachies, Ten Lectures on Wavelets (SIAM, Philadelphia, 1992).

[5] C. K. Chiu, An Introduction to Wavelets (Academic, San Diego, 1992).

[6] I. Daubechies, Commun. Pure Appl. Math. 41, 909 (1988).

[7] I. Daubechies, IEEE Trans Inf. Theory 36, 961 (1990).

[8] S. G. Mallat, Courant Institute of Mathematics, New York University, Technical Report No. 412 (unpublished).

[9] S. G. Mallat, IEEE Trans. Pattern Anal. Mach. Intell. 11, 674 (1989).

[10] G. Strang, SIAM Rev. 31, 614 (1989).

[11] P. Goupillaud, A. Grossmann, and J. Morlet, Geoexploration 23, 85 (1984/85).

[12] Wavelets, edited by J. M. Combes, A. Grossmann, and Ph. Tchamitchian (Springer-Verlag, New York, 1989).

[13] Wavelets and Their Applications, edited by M. B. Ruskai et al. (Jones and Bartlett, Boston, 1992).

[14] F. C. Moon and P. J. Holmes, J. Sound Vib. 65, 285 (1979); 69, 339 (1980).

[15] J. Guckenheimer and P. Holmes, Nonlinear Oscillations, Dynamical Systems, and Bifurcations of Vector Fields (Springer-Verlag, New York, 1983).

[16] A. J. Lichtenberg and M. A. Lieberman, Regular and Stochastic Motion (Springer-Verlag, New York, 1983).

[17] C. W. Gear, Numerical Initial Value Problems in Ordinary Differential Equations (Prentice-Hall, Englewood Cliffs, NJ, 1971); L. F. Shampire and M. H. Gordon, Computer Solution of Ordinary Differential Equations (Freeman, San Francisco, 1975).